

Surface barriers, irreversibility line, and pancake vortices in an aligned $\text{HgBa}_2\text{Ca}_2\text{Cu}_3\text{O}_{8+\delta}$ superconductor

Y. C. Kim*

Department of Physics, University of Tennessee, Knoxville, Tennessee 37996-1200

J. R. Thompson

*Department of Physics, University of Tennessee, Knoxville, Tennessee 37996-1200
and Solid State Division, Oak Ridge National Laboratory, P.O. Box 2008, Oak Ridge, Tennessee 37831-6061*

D. K. Christen

Solid State Division, Oak Ridge National Laboratory, P.O. Box 2008, Oak Ridge, Tennessee 37831-6061

Y. R. Sun†

Department of Physics, University of Tennessee, Knoxville, Tennessee 37996-1200

M. Paranthaman

Chemical and Analytical Sciences Division, Oak Ridge National Laboratory, P.O. Box 2008, Oak Ridge, Tennessee 37831-6100

E. D. Specht

Metals and Ceramics Division, Oak Ridge National Laboratory, P.O. Box 2008, Oak Ridge, Tennessee 37831-6118

(Received 28 November 1994)

The irreversible magnetic properties of a magnetically aligned $\text{HgBa}_2\text{Ca}_2\text{Cu}_3\text{O}_{8+\delta}$ superconductor have been investigated as a function of temperature and magnetic field, for both $\mathbf{H}\parallel c$ axis and $\mathbf{H}\parallel ab$ plane. Experimental results for the magnetic hysteresis ΔM , the field of first flux penetration H_p , and the irreversibility line with $\mathbf{H}\parallel c$ are well described by recent theory [L. Burlachkov *et al.*, Phys. Rev. B **50**, 16 770 (1994)] for thermally activated penetration of a surface barrier by pancake vortices. Near 85 K, the system crosses over from two-dimensional to three-dimensional line vortices, from which we extract estimates for the mass anisotropy parameter ϵ .

INTRODUCTION

Putilin *et al.*¹ first discovered superconductivity with a transition temperature T_c of 94 K in $\text{HgBa}_2\text{CuO}_{4+\delta}$, a Hg-based cupric oxide containing just one Cu-O layer per unit cell. Subsequently, Schilling *et al.*² discovered corresponding materials with more Cu-O layers per cell that became superconductive at $T_c=133$ K; the authors correctly interpreted that the mixed-phase material contained $\text{HgBa}_2\text{Ca}_2\text{Cu}_3\text{O}_{8+\delta}$, with three adjacent Cu-O layers in the unit cell. The relatively simple tetragonal structure and high transition temperatures of these new compounds generated much interest and possible alternatives to other high- T_c superconductors for technological usage. For many applications, however, the materials must be able to conduct large electric currents in the presence of high magnetic fields. In this work, we use magnetic studies to establish the limits of supercurrent conduction and interpret the results in terms of recent theory³ for tunneling of “pancake” vortices⁴ through a surface barrier. The experimental studies were performed on aligned grains of the three layer material, $\text{HgBa}_2\text{Ca}_2\text{Cu}_3\text{O}_{8+\delta}$. This enables us to obtain information on isolated grains of the superconductor, particularly with the field applied perpendicular to the Cu-O

planes. The procedure eliminates both intergranular current conduction and the complexity of angular averaging over grain orientations in random polycrystals.

To obtain further insight into the types of vortices present and their motion, we have studied the irreversibility line for both field orientations, $\mathbf{H}\parallel c$ and $\mathbf{H}\parallel ab$. Obviously, a high irreversibility field $H_{\text{irr}}(T)$ is a necessary (but not sufficient) condition for conducting large current densities in high magnetic fields. If coarsely characterized by a power law, the temperature dependence of $H_{\text{irr}}(T) \sim (1 - T/T_c)^n$ varies from one high- T_c family to another, with the exponent n lying between 1.5 and 5.5: for $\text{YBa}_2\text{Cu}_3\text{O}_7$,⁵ $n=1.5$; for $\text{HgBa}_2\text{CaCu}_2\text{O}_{6+\delta}$,⁶ $n=2.5$; and for $\text{Tl}_2\text{Ba}_2\text{Ca}_2\text{Cu}_3\text{O}_{10+\delta}$,⁷ and $\text{Bi}_2\text{Sr}_2\text{CaCu}_2\text{O}_8$,⁸ $n=5.5$. From such studies, Xu and Suenaga,⁸ concluded that $H_{\text{irr}}(T)$ is a depinning line rather than a lattice melting or glass-to-liquid phase-transition field, for example.

In the present work, study of the irreversibility line $H_{\text{irr}}(T)$ with the applied field $\mathbf{H}\parallel c$ axes gives substantial evidence for a mechanism based on creep of two-dimensional (2D) vortices through a surface barrier. Analyses of the width of the magnetic hysteresis loops and the temperature dependence of the field of first penetration corroborate this interpretation. Previously,

we observed significant surface barrier effects at low temperatures for a wide range of magnetic fields in random polycrystals of the $\text{HgBa}_2\text{CuO}_{4+\delta}$ (Hg-1201) compound⁹ and in polycrystals of Hg-1212 and Hg-1223 as well.¹⁰ We associated these effects with the surfaces of individual grains and this conclusion is substantiated by the presence of similar surface-related features in the current work on aligned powders. To date, few studies have been reported on aligned $\text{HgBa}_2\text{Ca}_2\text{Cu}_3\text{O}_{8+\delta}$ materials, which allows one to isolate the case in which the field is applied perpendicular to the Cu-O planes. Also, one can compare and contrast the properties with $\mathbf{H}\parallel c$ and with $\mathbf{H}\parallel ab$. Consequently, we examine the magnetization M , the magnetic hysteresis ΔM , and $H_{\text{irr}}(T)$ for these two field orientations.

EXPERIMENTAL ASPECTS

Bulk samples of $\text{HgBa}_2\text{Ca}_2\text{Cu}_3\text{O}_{8+\delta}$ were prepared by a solid-state reaction of stoichiometric mixtures of 99.998% HgO, 99.997% BaO, 99.97% CaO, and 99.999% CuO, as described previously.¹¹ The relatively high phase purity of the $\text{HgBa}_2\text{Ca}_2\text{Cu}_3\text{O}_{8+\delta}$ end product (>90% phase purity, as determined from x-ray diffractometry), makes it possible to obtain reliable information on this material.

Powder particles for the composite samples were made by hand grinding with a mortar and pestle inside a glove box. After passing through a 45 μm sieve, the powder was examined by scanning electron microscopy and its size distribution was measured using instrumentation based on light attenuation-precipitation rate methods.¹² To a good approximation, the size distribution followed the commonly observed log-normal form, i.e., a Gaussian with the logarithm of particle size as its argument. The mean particle diameter was $\langle d \rangle = 8 \mu\text{m}$ and the standard deviation in $\ln(d)$ was 0.5.

Powders of $\text{HgBa}_2\text{Ca}_2\text{Cu}_3\text{O}_{8+\delta}$ were dispersed in liquid epoxy and aligned in an applied magnetic field of 5 T at room temperature, using a procedure similar to that reported by Farrell *et al.*¹³ After solidification of the epoxy, the composite material was removed from its teflon mold and checked for alignment. As is evident in Fig. 1, x-ray diffraction confirmed a uniaxial alignment with the crystalline c axis parallel to the applied field, since only (00 l) reflections of Hg-1223 were observed for the scattering vector parallel to this direction. There are, however, two unidentified reflections near $2\theta = 35^\circ - 40^\circ$, but the d spacings do *not* correspond to $\text{HgBa}_2\text{Ca}_2\text{Cu}_3\text{O}_{8+\delta}$; thus they represent some unidentified impurity rather than misaligned superconductor. The full width at half maximum of the rocking curve for the (006) reflection was 2.6° (see inset to Fig. 1).

Measurements of the isothermal magnetization $M(H)$ were made for a set of temperatures T between 5 and 120 K, with field orientations $\mathbf{H}\parallel c$ and $\mathbf{H}\parallel ab$, using a Quantum Design model MPMS-7 superconducting quantum interference device-based magnetometer. Applied magnetic fields up to 6.5 T were used. Scan lengths of 3 cm, providing a field uniformity of <0.005% during measurement, were used, and temperature was stabilized to

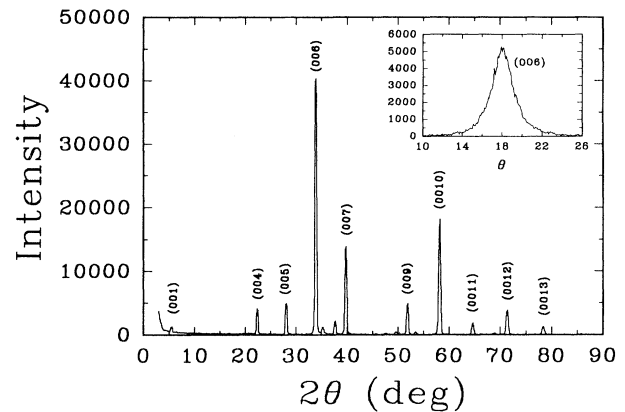


FIG. 1. The Cu K_α x-ray diffractogram for grain-aligned $\text{HgBa}_2\text{Ca}_2\text{Cu}_3\text{O}_{8+\delta}$, obtained with the scattering vector parallel to the alignment direction. The regularly spaced (00 l) reflections indicate c -axis alignment. Inset: the rocking curve for the (006) reflection.

within ± 0.05 K of the target temperature before application of the magnetic field. After each field increment, the system paused for 10 sec to allow fast instrumental transients to decay before measuring the magnetic moment. The magnetization $M = m/V$ is defined as the measured magnetic moment m per unit volume V of superconductor, as calculated from the mass and the theoretical density of the superconductor, $\rho_{x\text{ ray}} = 6.28 \text{ g/cm}^3$.

For studies of the superconductive transition in low magnetic fields, the 7 T superconducting magnet in the magnetometer was “reset” by heating it above its transition temperature. This procedure released the trapped magnetic flux in the magnet, so that small fields could be applied accurately.

THEORETICAL OVERVIEW

Recently, Burlachkov *et al.*³ treated the theoretical problem of giant flux creep through surface barriers in high-temperature superconductors. While traditional theory¹⁴ considered the transmission of a vortex *line* through a surface, the recent work particularly focuses on the 2D case of “pancake” vortices, as is appropriate when the interlayer coupling is small compared with other energies in the system. For the situation in which the magnetic field H is increased from zero, the pancakes cannot penetrate into the superconductor until the field reaches the penetration field, given by

$$H_p = H_c \exp[-T/T_0], \quad (1)$$

where H_c is the thermodynamic critical field and T is the temperature. Here the characteristic temperature is $T_0 = \epsilon_0 d / \ln(t/t_0)$ where “ d ” ≈ 1.6 nm is the spacing between sets of Cu-O planes, $\epsilon_0 = (\phi_0/4\pi\lambda)^2$ is the vortex line energy, ϕ_0 is the flux quantum, and t/t_0 is the ratio of the experimental time (since application of the field) to the fundamental time scale t_0 for vortex oscillations. At

$T=0$, the expression in Eq. (1) matches the traditional result that $H_p \approx H_c$; the exponential factor in Eq. (1) is a consequence of thermally activated creep of pancakes into the superconductor, which causes H_p to fall off much more rapidly with temperature than expected classically from $H_c(T)$. In practice, surface imperfections often reduce the magnitude of the prefactor in Eq. (1), but do not change the value of T_0 .

When one continues to increase the field beyond H_p , the magnetization M decreases. Furthermore, when the field is subsequently reduced, the magnetization is nominally field independent with $M \approx 0$. Consequently, the width of the magnetization loop for $H \gg H_p$ is

$$\Delta(4\pi M) \approx H_p^2/H \propto \exp(-2T/T_0), \quad (2)$$

which is a temperature dependence that can be tested readily. At sufficiently extreme field-temperature conditions, the pancake hopping distance becomes comparable with the thickness of the vortex-free surface layer.¹⁴ Then the penetration by pancakes becomes reversible and ΔM collapses to some resolution-limited level ΔM_{exp} . This serves to define the irreversibility line, which in the 2D case is given by

$$H_{\text{irr}} \approx H_{c2} \times (T_0/2T) \exp(-2T/T_0). \quad (3)$$

At high temperatures where the operative range of magnetic field is small, it is also possible that the coupling between pancake vortices successfully competes with other energies in the system, so that 3D line vortices form in the anisotropic superconductor. Then the theory predicts that the penetration field H_p is given

$$H_p \approx H_c \pi \epsilon \epsilon_0 \xi \ln^2(H_c/H_p) / [2^{3/2} T \ln(t/t_0)] \propto (1-t)^{3/2}, \quad (4)$$

where $\epsilon = (m/M)^{1/2} < 1$ is the mass anisotropy ratio and $t = T/T_c$ is the reduced temperature. Here and below, the last factor shows the dominant temperature dependence near T_c . With 3D line vortices, several different mechanisms may serve to define the irreversibility line. If single vortex hopping over a surface barrier dominates, then one has

$$H_{\text{irr}}^s \approx \pi \epsilon \epsilon_0 \phi_0 \ln^3(H_{c2}/H_{\text{irr}}^s) / [256 T^2 \ln^2(t/t_0)] \propto (1-t)^2. \quad (5)$$

Burlachkov *et al.*³ argue, however, this process is not possible very close to equilibrium, since it requires infinite energy. An alternative process near (but not *too* near) equilibrium is collective creep of a bundle of vortices into the system. Then one has

$$H_{\text{irr}}^{\text{col}} \approx H_{\text{irr}}^s \times [\phi_0 / (4\pi\lambda)^2]^2 / [\Delta M_{\text{exp}}]^2 \propto (1-t)^4. \quad (6)$$

Competing with these is conventional melting of the 3D vortex system, as given by the expression

$$B_m \approx 8\epsilon^2 \epsilon_0^2 c_L^4 \phi_0 / T^2 \propto (1-t)^2, \quad (7)$$

where $c_L \approx 0.2$ is the Lindemann melting factor. The field at which the vortex system crosses over from 2D to

3D behavior is given by the expression¹⁵

$$B_{\text{cr}} = [\phi_0 \epsilon^2 / \pi d^2] \ln\{(d/\epsilon \xi_{ab})/4[\ln(d/\epsilon \xi_{ab})]^{1/2}\}. \quad (8)$$

After presenting some more general results, we will use these various temperature dependencies to distinguish among the different processes. Most importantly, the comparisons will (1) demonstrate that surface barrier effects dominate the magnetic response of these aligned HgBa₂Ca₂Cu₃O_{8+ δ} materials and (2) provide substantial support for the validity of the theory just outlined.

RESULTS AND DISCUSSION

Characterization of the superconductive materials begins with its low-field magnetic response. Figure 2 shows the temperature dependence of the dc susceptibility $4\pi\chi$, measured in a static applied field $H_{\text{app}} = 4.0$ Oe. Here we define the dc susceptibility as $\chi = M/H_{\text{eff}}$, where $H_{\text{eff}} = (H_{\text{app}} - 4\pi DM)$ is the effective field that includes demagnetizing effects; for the approximately equiaxed particles of superconductor, the effective demagnetizing factor is $D \approx 1/3$. Zero-field-cooling (zfc) measurements consisted of cooling to 5 K in zero field, applying a 4 Oe measuring field, then warming to observe the resulting shielding signal as a function of temperature. After warming the sample above T_c , it was field cooled (fc) in the same 4 Oe to observe the Meissner signal (not shown).

The narrow transition shown in Fig. 2 illustrates the homogeneity of the sample. No significant structure, such as additional signals near 95 K due to a minority phase content of Hg-1201, is observed in the data. The conventional superconductive transition temperature T_c , defined by the low-field onset of diamagnetism, is 133.5 K. At low temperature, the zfc susceptibility for $\mathbf{H} \parallel c$ is $4\pi\chi = -0.94$, corresponding to nearly complete screening of the grains' interior; for $\mathbf{H} \parallel ab$, the corresponding zfc value is -0.26 . The Meissner signal due to ab -plane supercurrents was large, with a fc susceptibility $4\pi\chi = -0.76$ for $\mathbf{H} \parallel c$. At 5 K, the corresponding fc value with $\mathbf{H} \parallel ab$ was -0.17 .

The isothermal magnetic response (hysteresis loops) of the Hg-1223 material was studied in applied fields up to

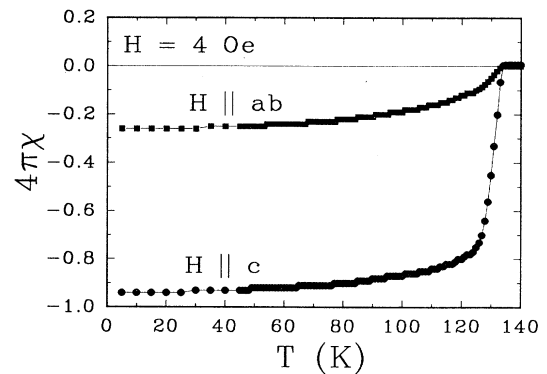


FIG. 2. The susceptibility $4\pi\chi$ versus temperature for aligned HgBa₂Ca₂Cu₃O_{8+ δ} , for $\mathbf{H} \parallel c$ and $\mathbf{H} \parallel ab$, after cooling in zero field. The data are corrected for demagnetizing effects.

6.5 T. An example is shown in Fig. 3, a plot of magnetization M versus H at $T = 15$ K for increasing and then decreasing field history. Results are shown for both field orientations. As we demonstrated earlier for randomly oriented polycrystals,^{9,10} the loops are quite asymmetric; the magnetic moment in the decreasing field branch is almost field independent with nearly zero magnitude. These features and others, such as the ac field dependence of the real and imaginary responses in audio frequency studies,⁹ give strong evidence for pronounced surface barrier effects in Hg-based cuprate superconductors in their as-formed condition.

One prominent feature of the ascending field branching in Fig. 3 is the distinct peak in M . We use this peak to locate the penetration field H_p : theoretically, penetration by pancakes is predicted to be an avalanche process, so that $|M|$ decreases steeply above H_p , as is observed. Initially, we test the dependence in Eq. (1) that $H_p \sim H_c \times \exp(-T/T_0)$ by making a semilogarithmic plot of the experimental values of $H_p(T)$ (open symbols) versus T in Fig. 4. An approximately exponential falloff is evident over a substantial temperature range. From the slope of the best fit to these data (solid line), we obtain the value $T_0 = 50$ K. Also, the intercept at $T = 0$ is 0.16 T. This is about 20% of the deduced¹⁶ thermodynamic critical field $H_c(0)$; the reduction is ascribed to surface imperfections in the superconducting grains.

As presented, this analysis treats H_c as a fixed quantity. Even in a classical superconductor, however, the field H_p [$\approx H_c(T)$] for penetration through a surface barrier decreases with temperature. One can account for this temperature dependence using the Ginzburg-Landau and two-fluid relation

$$H_c(T) = \phi_0 / [2^{3/2} \pi \xi(T) \lambda(T)] \\ = H_c(0) [(1-t^2)^{1/2} (1-t^4)^{1/2}]. \quad (9)$$

Including this additional factor, we plot as solid symbols in Fig. 4 the quantity $H_p \times (1-t^2)(1+t^2)^{1/2}$, which should fall off exponentially with T according to Eq. (1). The straight line through the data represents the theoretic

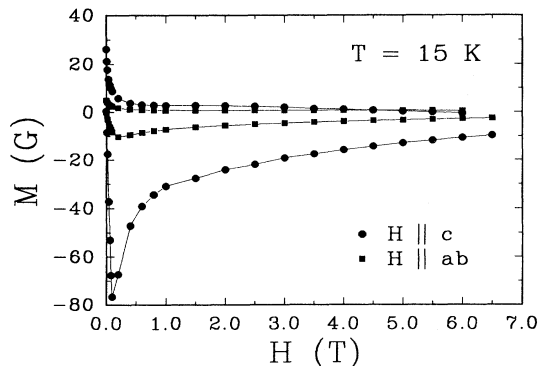


FIG. 3. Field dependence of the magnetization M at 15 K with $\mathbf{H} \parallel c$ (●) and $\mathbf{H} \parallel ab$ (■). The asymmetry and the flat decreasing field branch with $M \approx 0$ are due to surface barrier effects.

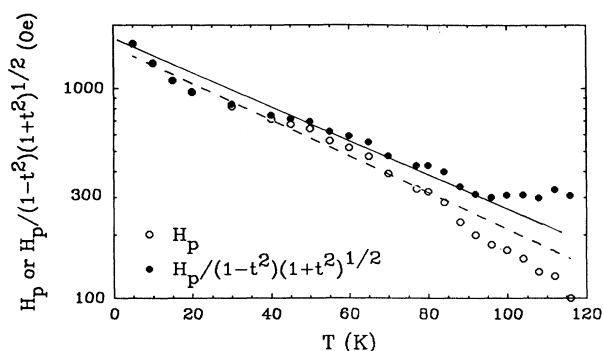


FIG. 4. Dependence of the field of first penetration $H_p \approx H_c \times \exp(-T/T_0)$ on temperature T . Open symbols show an analysis that assumes $H_c = \text{const}$. Including a temperature dependence for H_c gives the solid symbols; see text. The straight lines illustrate the exponential falloff of Eq. (1), which persists up to 85–90 K.

cal form, which is followed reasonably well up to ~ 85 K. The break and flattening of the curve at higher temperatures signifies an onset of new physics, which is discussed later following treatment of the irreversibility line. This analysis yields the value $T_0 = 59$ K for the characteristic temperature.

We now consider the hysteresis in the magnetization, which Fig. 3 shows is substantial. From detailed measurements of $M(H, T)$, one can construct the magnetic hysteresis $\Delta M = [M(H \text{ decreasing}) - M(H \text{ increasing})]$, for fixed values of field and temperature. To interpret these and following results, let us recall that hysteresis in the magnetization arises from the presence of macroscopic supercurrents in the grains of superconductor. One possibility is that currents flow only very near the surface of a grain, due to the presence of a surface barrier. A second possibility is that currents exist throughout the volume of a grain and are associated with a gradient in flux density, as embodied in the Bean critical-state model. Finally, current flow can be supported by a combination of these, in which vortex motion is inhibited by both bulk pinning and surface barrier effects, with the relative strengths of the two possibly depending on both field and temperature. In the present case, it is clear that surface effects dominate, while bulk effects play a secondary but sometimes nontrivial role. For example, the predicted field dependence $\Delta M \propto 1/H$ is followed imprecisely, a feature that we attribute to residual bulk effects at low temperature and to approaching the irreversibility line at high temperatures.

Experimental results for ΔM versus T are shown in Fig. 5 for applied fields of 1 and 2 T, for both field orientations. For the most part, we concentrate on the better understood and more reliable case with $\mathbf{H} \parallel c$, i.e., H perpendicular to the Cu-O planes. The linear behavior in Fig. 5 corresponds to an exponential temperature variation, which persists up to ~ 50 and 40 K, respectively, for $\mathbf{H} \parallel c$. This temperature dependence has precisely the form predicted by Eq. (2). The rate constant for the falloff gives the value $T_0 = 33$ K with $H = 1$ T [Fig. 5(a)]

and 26 K for $H=2$ T [Fig. 5(b)]. Note that $\Delta M \propto \exp(-2T/T_0)$ decreases much faster with T than does the penetration field H_p .

For moderate levels of magnetic field, the hysteresis ΔM with $\mathbf{H}\parallel c$ is about a factor of eight larger than that with $\mathbf{H}\parallel ab$. This anisotropy in ΔM is somewhat larger than that observed (4.5) in aligned $\text{HgBa}_2\text{CuO}_{4+\delta}$ at low field by Lewis *et al.*¹⁷ Before proceeding, let us recall the geometry for the two configurations. With $\mathbf{H}\parallel c$, the induced supercurrents flow in the Cu-O planes, with (line or pancake) vortex motion being driven in the poorly pinned a or b direction of the unit cell. In the alternative case with $\mathbf{H}\parallel ab$, the circulating currents flow *both* in the ab planes (with vortex motion along the intrinsically pinned c direction) and perpendicular to the planes (with vortex motion parallel to the planes, sliding between them). Thus the magnetization in the latter arrangement folds together two different current densities.

The anisotropy in magnetization ΔM changes with field and temperature. Compare, for example, the two curves in Fig. 5(a) for $\mathbf{H}\parallel c$ and $\mathbf{H}\parallel ab$. At low field and low temperature, ΔM is largest with $\mathbf{H}\parallel c$. However, when the magnitude of the field or the temperature increases sufficiently, the curves cross and the sense of the anisotropy reverses. With $H=1$ T, this occurs near 55 K, as seen in Fig. 5(a). The magnetic field at which the two cross decreases rapidly with temperature. This is shown in Fig. 6, a plot of the crossover field H^* versus temperature. Empirically, we see that the crossing field decreases almost exponentially with temperature. Similar

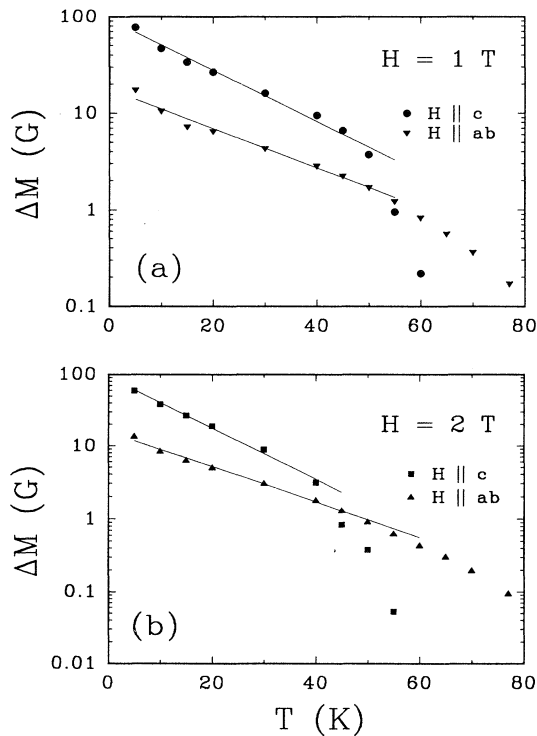


FIG. 5. Temperature dependence of the magnetic hysteresis ΔM for aligned $\text{HgBa}_2\text{Ca}_2\text{Cu}_3\text{O}_{8+\delta}$ with $\mathbf{H}\parallel c$ and $\mathbf{H}\parallel ab$ in applied fields of (a) 1 T and (b) 2 T.

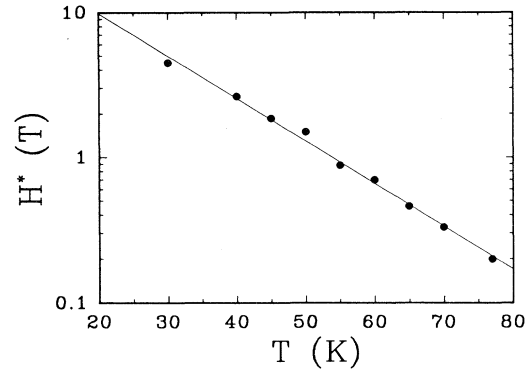


FIG. 6. Temperature dependence of the “crossing” field H^* , the field at which ΔM is the same for the two field orientations $\mathbf{H}\parallel c$ and $\mathbf{H}\parallel ab$. (See Fig. 5).

behavior was reported for $\text{HgBa}_2\text{CuO}_{4+\delta}$ materials, but the values are substantially higher in the present case: for Hg-1201 at 20 K, the crossover lies at 0.2 T,¹⁷ compared with an estimated 10 T at 20 K and 4.5 T at 30 K for $\text{HgBa}_2\text{Ca}_2\text{Cu}_3\text{O}_{8+\delta}$. (Our measurements on the Hg-1201 system give a crossing field close to that in Hg-1223, e.g., 4.3 T at 30 K. The reasons for these variations in properties are unknown.)

Thus far, we have considered two topics, the field $H_p(T)$ at which pancake vortices first surmount the surface barrier and the temperature dependence of the irreversible magnetization ΔM . Now we examine the irreversibility line (IL), the boundary in the H - T plane at which $\Delta M \rightarrow 0$. With a surface barrier, this condition corresponds to reversible movement of pancakes or line vortices through the surface; with bulk pinning, it corresponds to a vanishing of the persistent current density. Experimentally, we define the IL as the field at which the isothermal ΔM decreases to some minimum value ΔM_{exp} , here 0.02 G, which is near the noise floor for measurements. This level lies near the baseline in Figs. 5(a) and 5(b). The results for H_{irr} are shown in Fig. 7 for the two field orientations. As is normally the case, the IL lies much higher when the field is applied parallel to the Cu-O planes. If one coarsely characterizes the entire temperature dependence via a power law $H_{\text{irr}} \propto (1 - T_{\text{irr}}/T_c)^n$, as shown by Welp *et al.*,¹⁸ then we obtain $n \approx 5$ in this case. Before analyzing these data in more detail, we note that the data of Schilling *et al.*¹⁹ on random polycrystals fall approximately midway in temperature between our measurements with the two field orientations.

Since surface barrier effects seem to dominate many other features of these Hg-based materials, let us now analyze the irreversibility line from this perspective. For the 2D case with pancake vortices, Eq. (3) provides an approximately exponential dependence on T . In the following analysis, we use the simple relation $H_{c2}(T) = H_{c2}(0)[1 - t^2]$ to account for its relatively minor temperature dependence. Consequently, plotting the quantity $H_{\text{irr}}T/[1 - t^2]$ on a logarithmic axis versus T should render a linear representation of the data. The resulting

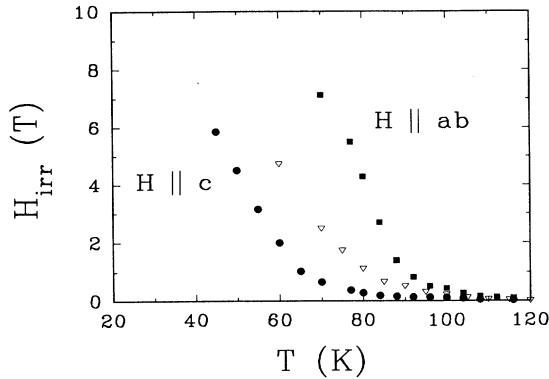


FIG. 7. The irreversibility line $H_{\text{irr}}(T)$ in aligned $\text{HgBa}_2\text{Ca}_2\text{Cu}_3\text{O}_{8+\delta}$ with $\mathbf{H}\parallel c$ and $\mathbf{H}\parallel ab$. Open symbols show the data of Schilling *et al.* (Ref. 19) acquired on polycrystalline materials.

plot, Fig. 8, shows that the 2D theoretical relation Eq. (3) describes the measurements at low and intermediate temperatures relatively well. Near 80–85 K, there is a distinct break, signifying the onset of some new regime. From the slope of the straight line in Fig. 8, we obtain the value $T_0 = 31$ K. Also, fitting Eq. (3) gives the rough estimate $H_{c2}(0) \sim 410$ T. This value is larger by a factor of 2.7 than the result $H_{c2}(0) = 150$ T obtained from an analysis of the equilibrium magnetization of this aligned material.¹⁶ The reason for the discrepancy is not known, but it may originate similarly to the theoretical overestimate³ of activation energies by comparable factors of 2–3.

At high enough temperatures and sufficiently small fields, the vortex pancakes should couple into vortices and form an anisotropic 3D system. Then $H_{\text{irr}}(T)$ should change over to a power law of the form $[1-t]^n$, as shown in Eqs. (5)–(7). We identify this crossover with the break near 85 in Fig. 8. Figure 9 shows a standard analysis for a power-law dependence, a double logarithmic plot of

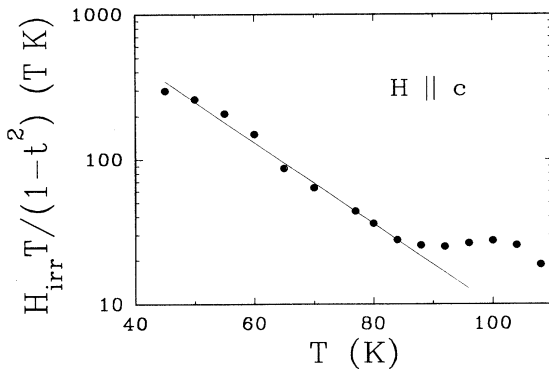


FIG. 8. Analysis of the irreversibility line for $\mathbf{H}\parallel c$, based on creep of pancake vortices through a surface barrier. The theory, Eq. (3) (straight solid line), describes the data well up to the 2D to 3D crossover near 85 K.

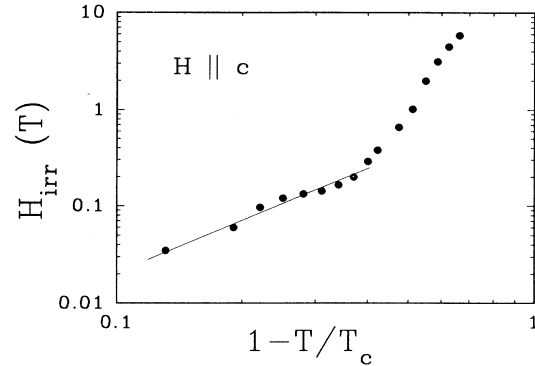


FIG. 9. The irreversibility line analyzed as a power law $H_{\text{irr}} \propto (1-T/T_c)^n$ at high temperature, as appropriate for 3D line vortices. The straight line has a slope $n = 1.7$; see text.

H_{irr} versus $[1-t]$. On this plot, the relationship is linear at high temperatures and persists down to ~ 80 K. The slope of the high-temperature segment gives an exponent $n = 1.7$. Thus we can rule out collective creep of vortex bundles as the active mechanism in this regime, since Eq. (5) has an exponent $n = 4$ that is much too large. The observed value is close to (but not exactly equal to) the power $n = 2$ predicted both for single vortex hopping over a surface barrier [Eq. (4)] and for conventional melting [Eq. (6)]. Since the former process requires infinite energy when the vortex system is close to equilibrium, conventional 3D melting remains as a viable explanation. With melting, exponents $n = 2$ have been observed close to T_c in very clean systems.²⁰ Rather commonly, however, values $n < 2$ have been observed, as summarized recently by Blatter and Ivlev.²¹ Their theoretical work shows that quantum fluctuations lead to a more complex functional dependence that can be approximated by a power law with reduced exponents, e.g., $n \approx 1.3-1.5$ for $\text{YBa}_2\text{Cu}_3\text{O}_7$. However, more weakly coupled, layered materials (such as that studied here) have enhanced thermal fluctuations, which reduces the relative importance of quantum effects and moves the effective exponent closer to 2. Hence the present value $n = 1.7$, which pertains to a moderately anisotropic material at temperatures significantly below T_c , lies plausibly between the case with pure thermal fluctuations very near T_c (for which $n = 2$) and the strongly reduced case with pronounced quantum fluctuation effects (for which $n = 1.3-1.5$). An alternative explanation for the observed disappearance of magnetic irreversibility is thermal activation of vortices from bulk pinning sites. This can give several different temperature dependencies, depending on the volume of the pinning site.

In the earlier discussion of the penetration field H_p , we noted that it too exhibits a change of character near 85 K. For $T \geq 90$ K, the data for $H_p \times (1-t^2)(1+t^2)^{1/2}$ in Fig. 4 (solid symbols) change little with temperature. This indicates that we have $H_p(T) \propto (1-t)^n$, with exponent $n \sim 1$. A more detailed power-law analysis like that in Fig. 9 shows that $n \approx 0.8$, which is smaller than the predicted value of $3/2$ in Eq. (4).

DISCUSSION

Many features of the experimental data are explained by surface barrier effects. Previously documented^{9,10} were (1) the asymmetric shape of the hysteresis loops, (2) details of the ac magnetic response, and (3) different rates of flux creep for the ascending field branch of the hysteresis loop compared with the decreasing field branch. Here we show good agreement with the predicted temperature dependence of the first entry field H_p for penetration by pancake vortices, Eq. (1). This analysis yields the value $T_0 = 50\text{--}59$ K for this characteristic temperature. In addition, the magnetic hysteresis ΔM exhibits an exponential temperature falloff as predicted by Eq. (2), with values $T_0 = 33$ and 26 K for applied fields of 1 and 2 T, respectively. A third test of the theoretical predictions and evaluation of this parameter comes from the irreversibility line at low temperatures, which is well described by the relation Eq. (3) for 2D pancake vortices. This analysis yields the result $T_0 = 31$ K. From the theory of Burlachkov *et al.*,³ one has $T_0 = \epsilon_0 d / \ln(t/t_0) \approx 36$ K, which agrees reasonably well with the experimental determinations. In evaluating this expression, we use the value $\lambda_{ab} = 170$ nm for the ab plane magnetic penetration depth obtained from studies of the equilibrium magnetization^{22,16} and set $\ln(t/t_0) \approx 30$, as noted theoretically³ and found experimentally for Y-Ba-Cu-O crystals by analyzing the persistent current density.²³ Comparison of these results shows not only the predicted temperature dependencies, but fair consistency in the values of the characteristic temperature T_0 . It is curious that the deduced values for T_0 qualitatively tend to increase for measurements conducted at higher temperatures and/or lower magnetic fields, but the theory provides no obvious sources for such an effect.

Over a large range of temperature, the irreversibility line exhibits 2D behavior. It has a distinct change of character near 85 K, above which the vortex system appears to be three dimensional. At the crossover, we have $H_{irr} \approx 0.2$ T. Theoretically, this occurs at a field $B_{cr} \sim \epsilon^2 \phi_0 / d^2$, where Eq. (8) gives the full expression. Solving the latter equation for the mass anisotropy parameter gives the estimate $\epsilon \approx 1/50$. By assuming that 3D melting governs H_{irr} at high temperature, which is consistent with its temperature dependence, one can obtain an alternative estimate for ϵ using Eq. (6). This procedure gives $\epsilon \approx 1/75$ to $1/35$, as based on typical values $c_L = 0.2$ to 0.3 for the Lindemann factor,²¹ respectively. The resulting values for ϵ are relatively small, smaller than the earlier estimate $\epsilon \leq 1/16$ of Couach *et al.*²⁴ that were based on ac response studies of mixed-phase, randomly oriented materials. In the study, the authors deduced a 2D to 3D crossover field of ~ 1 T, but stated that

the field could be as small as 0.2 T, which actually coincides with our value. Finally, note that the present estimate relies only on experimental studies with $\mathbf{H} \parallel c$, which is insensitive to any misalignment effects or angular distributions that can plague studies with $\mathbf{H} \parallel ab$. Further estimates of this important parameter will come when single crystals of Hg-1223 become available.

CONCLUSIONS

Powders of $\text{HgBa}_2\text{Ca}_2\text{Cu}_3\text{O}_{8+\delta}$ were dispersed and magnetically aligned in epoxy to produce uniaxially oriented material. Experimental results for the field of first penetration H_p , the magnetic hysteresis ΔM , and the irreversibility line H_{irr} with $\mathbf{H} \parallel c$ follow many predictions for giant creep of pancake vortices through a surface barrier. The temperature dependencies are well described in terms of the characteristic temperature T_0 . Its value as predicted by the theoretical expression using independently determined experimental parameters lies near the experimental values obtained from analysis of ΔM and H_{irr} . Given the cumulative agreement with theory based on 2D vortices, one concludes that tunneling of pancake vortices dominates the vortex dynamics at low and intermediate temperatures in this material. At high temperatures, the system crosses over to a 3D line vortices and behaves in a fashion reasonably described by 3D melting relations. Assuming 3D melting provides the estimate $\epsilon \approx 1/35\text{--}1/70$ for the mass anisotropy parameter. With $\mathbf{H} \parallel ab$, the magnetic hysteresis ΔM decreases more slowly as a function of field and temperature, and the irreversibility line lies at considerably higher temperature, compared with the better understood case with $\mathbf{H} \parallel c$ axes. Overall, these results constitute a clear example of giant flux creep of pancake vortices through a surface barrier with a crossover to line vortices at higher temperatures, and provide considerable support for the underlying theory.

ACKNOWLEDGMENTS

We wish to thank L. Burlachkov for theoretical communications and acknowledge useful discussions with J. A. Lewis and J. Schwartz. A portion of the work of J.R. T. was supported by the Science Alliance at The University of Tennessee, Knoxville. The research was sponsored by the Division of Materials Sciences, U. S. Department of Energy and technology development was funded by the Oak Ridge Superconducting Technology for Electric Energy Systems Program, Advanced Utility Concepts Division, Conservation and Renewable Energy Program, U.S. Department of Energy, both under Contract No. DE-AC05-84OR21400 with Martin Marietta Energy Systems, Inc.

*Permanent address: Department of Physics, Pusan National University, Pusan 609-735, South Korea.

†Present address: National High Magnetic Field Laboratory, Tallahassee, Florida.

¹S. N. Putilin, E. V. Antipov, O. Chmaissem, and M. Marezio, *Nature* (London) **362**, 226 (1993).

²A. Schilling, M. Cantoni, J. D. Guo, and H. R. Ott, *Nature* (London) **363**, 56 (1993).

- ³L. Burlachkov, V. B. Geshkenbein, A. E. Koshelev, A. I. Larkin, and V. M. Vinokur, *Phys. Rev. B* **50**, 16 770 (1994).
- ⁴John R. Clem, *Phys. Rev. B* **43**, 7837 (1991).
- ⁵Y. Yeshurun and A. P. Malozemoff, *Phys. Rev. Lett.* **60**, 2202 (1987).
- ⁶Z. J. Huang, Y. Y. Xue, R. L. Meng, and C. W. Chu, *Phys. Rev. B* **49**, 4218 (1994).
- ⁷V. K. Chan and S. H. Liou, *Phys. Rev. B* **45**, 5547 (1992).
- ⁸Y. W. Xu and M. Suenaga, *Phys. Rev. B* **43**, 5516 (1991).
- ⁹Yang Ren Sun, J. R. Thompson, H. R. Kerchner, D. K. Christen, M. Paranthaman, and J. Brynstad, *Phys. Rev. B* **50**, 3330 (1994).
- ¹⁰Y. R. Sun, J. R. Thompson, J. Schwartz, D. K. Christen, Y. C. Kim, and M. Paranthaman, *Phys. Rev. B* **51**, 581 (1995).
- ¹¹M. Paranthaman, *Physica C* **222**, 7 (1994).
- ¹²The particle size distribution was determined using a Horiba model LA-700 instrument.
- ¹³D. E. Farrell, B. S. Chandrasekhar, M. R. DeGuirre, M. M. Fang, V. G. Kogan, J. R. Clem, and D. K. Finnemore, *Phys. Rev. B* **36**, 4025 (1987).
- ¹⁴J. R. Clem, in *Proceedings of the 13th Conference on Low Temperature Physics (LT 13)*, edited by K. D. Timmerhaus, W. J. O'Sullivan, and E. F. Hammel (Plenum, New York, 1974), Vol. 3, p. 102.
- ¹⁵L. N. Bulaevskii, M. Ledvij, and V. G. Kogan, *Phys. Rev. Lett.* **68**, 3773 (1992).
- ¹⁶Y. C. Kim, J. R. Thompson, J. G. Ossandon, D. K. Christen, and M. Paranthaman, *Phys. Rev. B* **51**, 11 767 (1995).
- ¹⁷J. A. Lewis, C. E. Platt, M. Wegmann, M. Teepe, J. L. Wagner, and D. G. Hinks, *Phys. Rev. B* **48**, 10 (1993).
- ¹⁸U. Welp, G. W. Crabtree, J. L. Wagner, and D. G. Hinks, *Physica C* **218**, 373 (1993).
- ¹⁹A. Schilling, O. Jeandupeux, J. D. Guo, and H. R. Ott, *Physica C* **216**, 6 (1993).
- ²⁰R. G. Beck, D. E. Farrell, J. P. Rice, D. M. Ginsberg, and V. G. Kogan, *Phys. Rev. Lett.* **68**, 1594 (1992).
- ²¹G. Blatter and B. Ivlev, *Phys. Rev. Lett.* **70**, 2621 (1993).
- ²²Myoung-Kwang Bae, M. S. Choi, Mi-Ock Mun, Sergey Lee, Sung-Ik Lee, and W. C. Lee, *Physica C* **228**, 195 (1994).
- ²³J. R. Thompson, Yang Ren Sun, L. Civale, A. P. Malozemoff, M. W. McElfresh, A. D. Marwick, and F. Holtzberg, *Phys. Rev. B* **47**, 14 440 (1993).
- ²⁴M. Couach, A. F. Khodar, R. Calemczuk, Ch. Marcenat, J.-L. Tholence, J. J. Capponi, and M. F. Gorius, *Phys. Lett. A* **188**, 85 (1994).